PROCEEDINGS OF SCIENCE

LHCb inputs to astroparticle physics

Giacomo Graziani[*†]
INFN, Sezione di Firenze
E-mail: graziani@fi.infn.it

The LHCb experiment has distinctive features, providing novel possibilities for production measurements needed to improve the interpretation of cosmic ray observations in the space or through atmospheric showers. In particular, LHCb has the unique possibility, among the LHC experiments, to be operated in fixed-target mode using its internal gas target. The energy scale achievable at the LHC, the different available nuclear targets and the excellent detector capabilities for vertexing, tracking and particle identification offer unique opportunities. Using a helium target, the first measurement of antiproton production in proton-helium collisions was achieved using a 6.5 TeV proton beam, for antiproton energies in the range 12-110 GeV. The results are particularly relevant to the interpretation of the recent precise measurements of the antiproton flux in cosmic rays.

European Physical Society Conference on High Energy Physics - EPS-HEP2019 -
10-17 July, 2019
Ghent, Belgium

[*]Speaker.
[†]on behalf of the LHCb collaboration

PoS(EPS-HEP2019)039

1. Introduction

In the last years, experimental astroparticle physics entered a precision era with a variety of probes, calling for an improved understanding of interactions of cosmic rays during their propagation. A notable example is the atmospheric contribution to the flux of neutrinos at the PeV scale, requiring the understanding of charm production at the highest available energies. The background to dark matter searches through cosmic antimatter and to gamma astronomy is due to secondary production of antimatter particles and gamma rays in collisions between primary cosmic rays and the interstellar medium (ISM). Production cross-sections for the related processes are thus key ingredients to the interpretation of these measurements. The study of mass composition of primary cosmic rays at ultra-high energy through extensive atmospheric showers also requires accurate models of hadron-nucleus interactions in non-perturbative regime over a wide range of projectile energy, from 10^{12} down to 10 GeV. For all these cases, accelerator data are much needed to complement the experimental efforts on cosmic rays.

The LHCb experiment [1] has been conceived with the main goal of studying heavy flavour physics in pp collisions at the LHC. The distinctive features of the detector are the forward geometry, covering the pseudorapidity region $2 < \eta < 5$, and the excellent vertexing, tracking and particle identification capabilities, optimised for the reconstruction of heavy flavour decays. Another key feature is the online selection system, consisting of a hardware level with high output bandwidth (up to 1 MHz), followed by a software level providing high flexibility. LHCb has also the unique possibility, among the LHC experiments, to be operated in fixed target mode, using its internal gas target SMOG, through which a small quantity of noble gas (He, Ne and Ar) can be injected in the LHC vacuum (the target pressure is of order 10^{-7} mbar). The forward geometry of the detector is well suited to reconstruct the resulting beam-gas collisions, occurring at a nucleon-nucleon center-of-mass energy $\sqrt{s_{\rm NN}}$ up to 110 GeV.

These features provide possibilities for novel measurements of interest to the cosmic ray community. We discuss in the following results for charm production, both in beam-beam and beam-gas mode, and for antiproton production in pHe collisions. Prospects for other measurements are also reviewed.

2. Charm production

Neutrinos produced in atmospheric showers from the decay of charmed particles constitute a background to the observation of astrophysical neutrinos at the PeV scale, recently observed by the IceCube experiment [2]. LHCb data provide measurements in the forward direction at the highest energy available at accelerators. Exclusive measurements of D^0, D^+, D_s^+, D^* and Λ_c^+ hadrons in pp and pPb collisions with energy $5 \leq \sqrt{s_{\rm NN}} \leq 13$ TeV were released [3, 4, 5, 6, 7, 8].

Data are remarkably more precise than theoretical predictions, notably at low $p_{\rm T}$, as illustrated in Fig. 1. Therefore, they constitute a key input to the PDF fits and the resulting predictions for the atmospheric high-energy neutrino flux, as those performed by the PROSA collaboration [9].

Measurements in fixed target mode provide a much lower energy scale, $\sqrt{s_{\rm NN}} \sim 100$ GeV, but give access to large Bjorken-x values in the target nuclei. Charm production in this regime could be enhanced by the contribution of intrinsic charm, which is poorly constrained due to the current

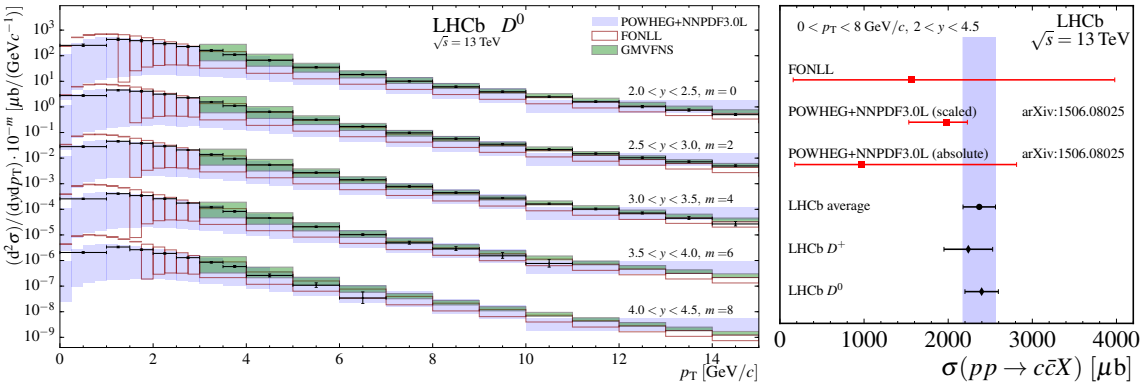

Figure 1: Example of charm production measurement in pp collisions [4]. The left plot shows the double differential cross-section in rapidity and transverse momentum for D^0 production at $\sqrt{s} = 13$ TeV. The right plot shows the resulting $c\bar{c}$ cross-section in the LHCb acceptance. Data are compared with theoretical predictions.

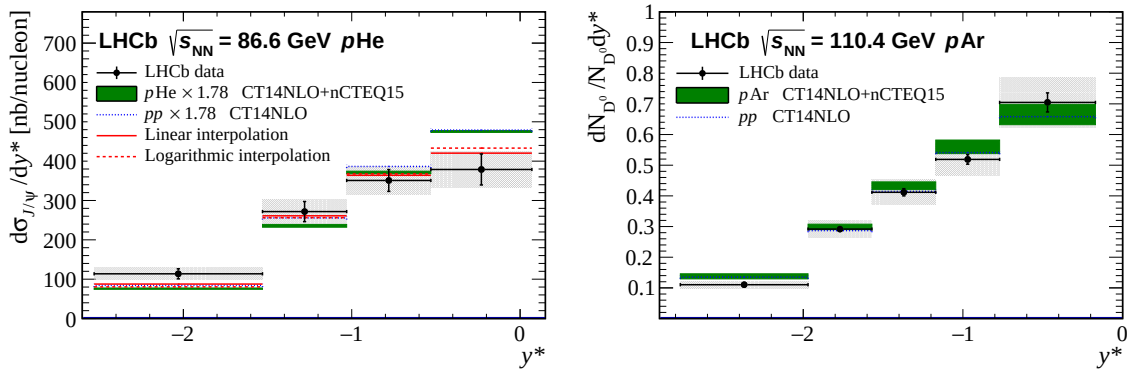

Figure 2: Distribution of rapidity in the centre-of-mass system for (left) J/ψ in pHe collisions and (right) D^0 in pAr collisions [10]. Data are compared to predictions from phenomenological models, normalised to data.

large uncertainties on the charm PDF at large x. LHCb released the first measurement of charm production from fixed-target data at the LHC [10]. The cross-sections for J/ψ and D^0 production are measured from samples of about 400 $J/\psi \to \mu^+\mu^-$ and about 2000 $D^0 \to K\pi$ decays, reconstructed from pHe collisions at $\sqrt{s_{NN}} = 86$ GeV, corresponding to an integrated luminosity of 7.6 ± 0.5 nb^{-1}. Differential shapes could be measured also from samples of similar size obtained from a a few nb^{-1} of pAr collisions (in this case, the luminosity could not be determined precisely). As shown in Fig. 2, the rapidity distribution is compatible with predictions not including an intrinsic charm contribution, which would enhance production at the most backward rapidities, corresponding to x values up to 0.4.

3. Antiprotons from pHe collisions

The prompt antiproton production in the pHe sample at 110 GeV has also been measured [11]. This study is motivated by the recent precision measurements performed in space, notably by AMS-

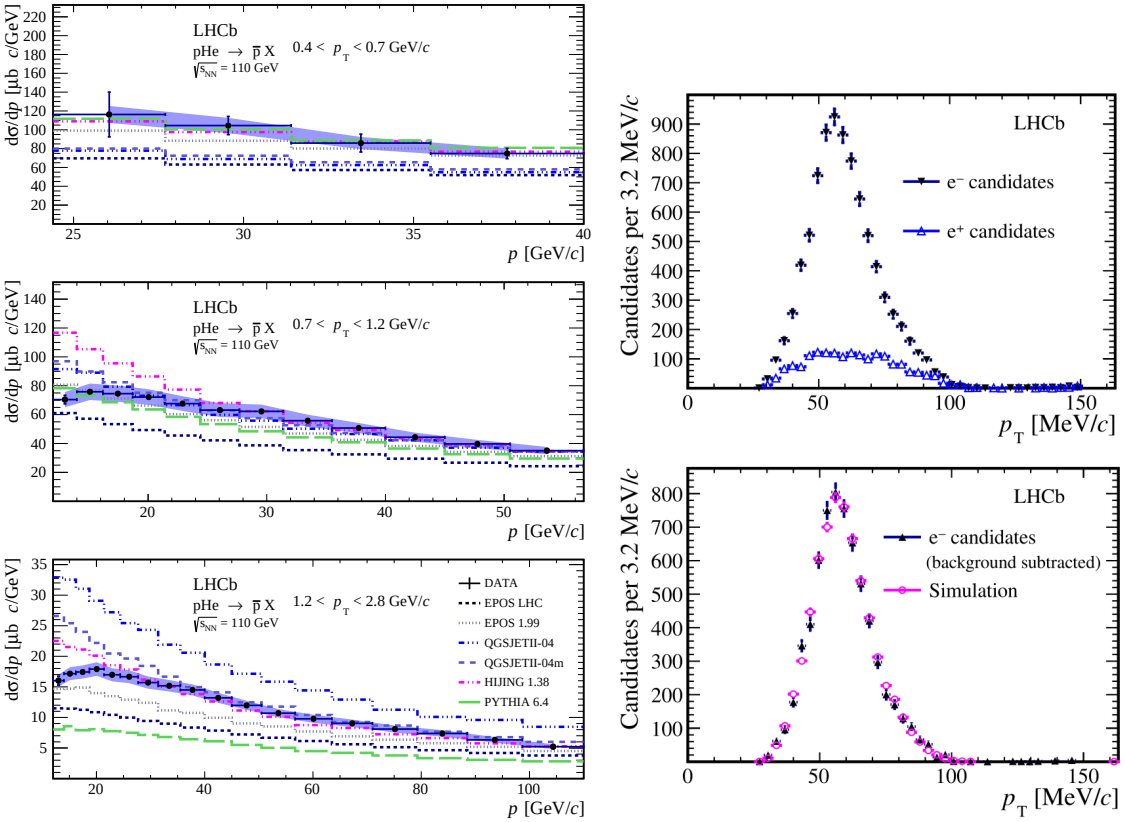

Figure 3: On the left plot, result for antiproton production in pHe collisions at 110 GeV. The differential production cross-section $d\sigma/dp$ is shown as a function of the momentum p for different ranges of p_{T} and is compared with several generators included in the CRMC package [13]. The normalization is obtained from the pe^- elastic scattering events from the same sample, illustrated in the right plots. The upper plot shows the p_{T} distribution for single scattered electron candidates with negative and positive charge, the latter sample being used to subtract the background from hadronic collisions. After subtraction, the distribution is found to agree well with the expected one from simulated pe^- scattering, as shown in the lower plot.

02 [12], of the antiproton content in cosmic rays, which is sensitive to possible exotic contributions like dark matter annihilation. For antiprotons above 10 GeV, the largest uncertainty on the expected flux of secondary antiprotons, produced during cosmic ray propagation in the ISM, is due to the limited knowledge of the corresponding production cross-sections. LHCb performed the first $\overline{p}$ production measurement in pHe collisions, which are responsible for about 40% of the expected cosmic $\overline{p}$ flux. The measurement was performed during a dedicated run in May 2016 using a sample of events acquired with minimum-bias online selection requirements. The particle identification capabilities of LHCb provide good antiproton identification in the momentum range between 12 and 110 GeV, which overlaps well the capabilities of the PAMELA and AMS-02 spectrometers. The detector acceptance covers particle with transverse momentum down to 400 MeV, and the measurement was performed in narrow kinematic bins.

Since the target gas pressure is not precisely known, the integrated luminosity of the fixed target samples is estimated from the yield of elastically scattered electrons from the target atoms. The

yield is determined by selecting events with a single low-pt track in the detector, identified as an $e^{\pm}$. The background to this normalization channel is due to soft diffractive collisions with a single track reconstructed in the detector and is expected to be symmetric in charge, so that it can be estimated and subtracted using the e^{+} candidates, as illustrated in Figure 3. The integrated luminosity is determined using this method with an accuracy of 6%, dominated by the systematic uncertainty on the electron reconstruction efficiency. This turns out to be the most limiting systematic uncertainty on the $\overline{p}$ cross-section measurement.

The results, also shown in Figure 3, are significantly more precise than the spread among the predictions from different phenomenological models, and are contributing to improve the models for the production cross-section of cosmic secondary antiprotons [14, 15]. Including the LHCb results in the fits is particularly important to parametrise scaling violations in the energy evolution of the invariant cross-section. The latest computations for the secondary $\overline{p}$ flux predictions using the updated parametrisations, and also taking profit of new pp data from NA61 and other improvements in the analysis, lead to a substantial improvement in accuracy for the flux prediction. The central values are now closer to the experimental measurements, reducing the significance of a possible excess of antimatter [16, 17].

4. Prospects

The measurements presented above are expected to be developed by exploiting the available fixed-target samples collected during the LHC Run 2. The largest one consists of pNe collisions, with an integrated luminosity of about 100 nb^{-1}, providing an additional order of magnitude in

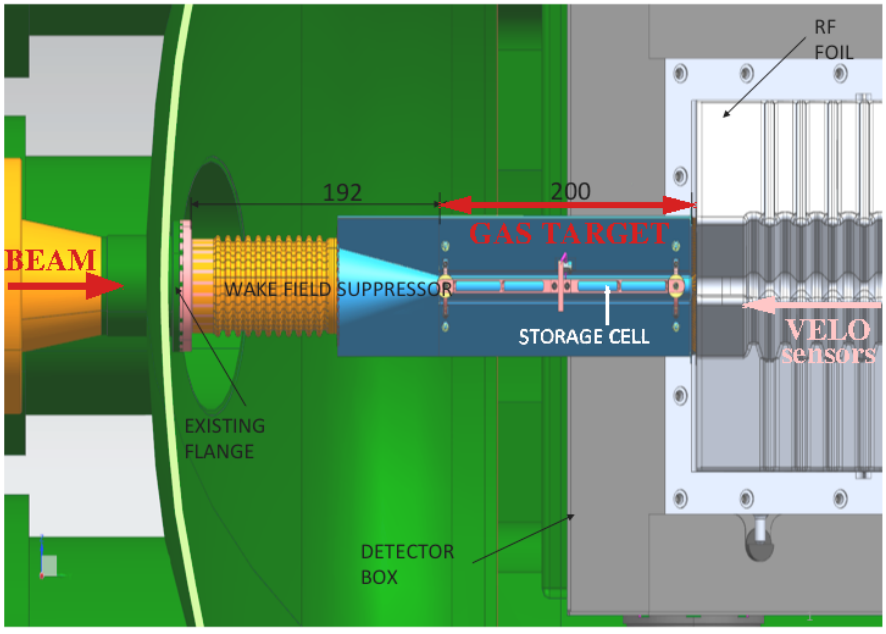

Figure 4: Sketch of the upgraded gas target, integrated in the design of the new vertex detector (VELO). As the rest of the VELO, the gas storage cell, which has an inner radius of 5 mm, is made of two retractable halves, which are closed only when stable beams are declared by the machine.

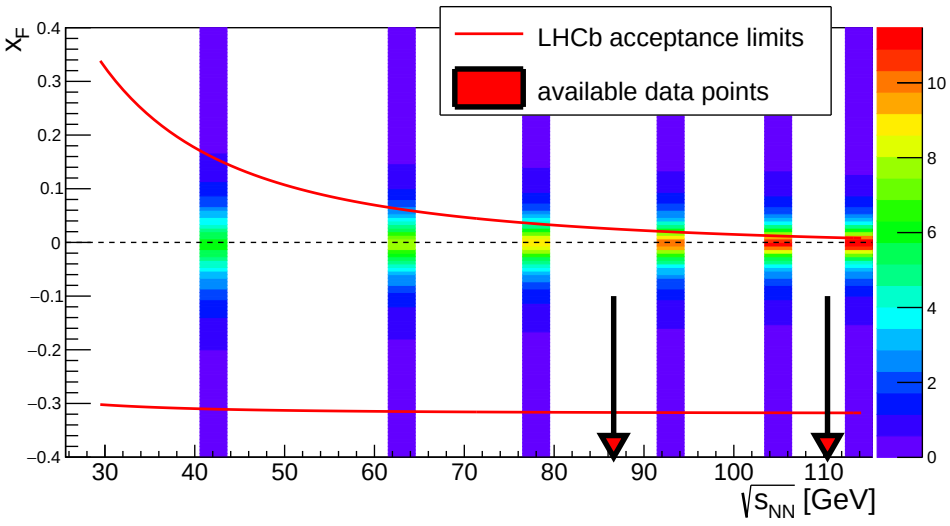

Figure 5: The graph shows the expected Feynman-x, x_F, probability density function for antiprotons with momentum between 12 and 110 GeV, produced in pHe collisions at different c.m. energies, according to the QGSJETII04m model [18]. The two thick lines indicate the minimum and maximum values of x_F accessible to LHCb for antiprotons with p_T below 2 GeV.

statistics for charm production studies, which could be extended to other states as the Λ_c^+ baryon. The sample of pHe collision at 86 GeV will be used to study the energy evolution of the $\overline{p}$ cross-section, and the secondary production of antiprotons due to anti-hyperon decays will be included in these studies. Production studies will be extended to the other light hadrons, to constrain the positron production in the ISM.

Additional possibilities are expected from the next LHC runs, taking profit of the currently ongoing detector upgrade [19] and notably of an upgraded target device [20], called SMOG2. This will consist of a storage cell containing the injected gas into a 20 cm long region located just upstream the LHCb vertex detector, as depicted in Fig. 4. The upgraded detector is expected to start data-taking in 2021. An increase in fixed-target luminosity by up to two orders of magnitude with the same injected gas flow is anticipated. Furthermore, it may be possible to inject more gas species, notably hydrogen and deuterium, providing pp reference for the other fixed-target samples.

The largest remaining uncertainties on the cosmic antiproton cross-sections could be addressed by this program. Measurements with hydrogen, deuterium and helium with the same detector are planned, providing accurate determinations of ratios. This will constrain nuclear effects in helium and isospin violations affecting the prediction for antineutron production, accounting for about half of the cosmic $\overline{p}$ flux. A scan in beam energy would provide accurate constraints on scaling violations and extend the detector acceptance toward positive values of Feynman-x, which are not covered at the highest LHC beam energy (see Fig. 5).

It is also planned to reproduce proton collisions in the atmosphere, by injecting nitrogen and possibly oxygen in SMOG2. Measurements of baryon and kaon production in pN and pO at $\sim$ 100 GeV would provide valuable inputs to solve the puzzle of off-axis muon production in extensive showers [21]. The possibility of circulating beams of oxygen ions during Run 3 is also being discussed. This would allow to study pO collisions up to $\sqrt{s_{\rm NN}} = 9.9$ TeV in the LHCb

forward acceptance. Furthermore, using an hydrogen target in SMOG2, one would have access to very forward particles, up to $\eta = 7.6$, in the projectile rest frame (pO collisions at $\sqrt{s_{\rm NN}} \sim$ 100 GeV).

In conclusion, a program of production studies relevant to cosmic ray physics is developing at LHCb, also thanks to a fruitful collaboration with the astroparticle community. With the upgraded gas target being installed for the LHC Run 3, several novel possibilities are expected in the near future.

References

[1] A. A. Alves Jr *et al.* (LHCb collaboration) *JINST* **3** (2008) S08005

[2] M. G. Aartsen *et al.* (IceCube collaboration) Science **342** (2013) 1242856

[3] R. Aaij *et al.* (LHCb collaboration) Nucl. Phys. **B871** (2013) 1

[4] R. Aaij *et al.* (LHCb collaboration) JHEP **03** (2016) 159, Erratum ibid. **09** (2016) 013, Erratum ibid. **05** (2017) 074

[5] R. Aaij *et al.* (LHCb collaboration) JHEP **06** (2017) 147

[6] R. Aaij *et al.* (LHCb collaboration) JHEP **10** (2017) 090

[7] R. Aaij *et al.* (LHCb collaboration) JHEP **08** (2018) 008

[8] R. Aaij *et al.* (LHCb collaboration) JHEP **02** (2019) 102

[9] M. V. Garzelli *et al.* (PROSA collaboration) JHEP **05** (2017) 004

[10] R. Aaij *et al.* (LHCb collaboration) Phys. Rev. Lett. 122 (2019) 132002

[11] R. Aaij *et al.* (LHCb collaboration) Phys. Rev. Lett. **121** (2018) 222001

[12] M. Aguilar *et al.* (AMS Collaboration) Phys. Rev. Lett. **117** (2016) 091103

[13] T. Pierog, C. Baus and R. Ulrich, CRMC (Cosmic Ray Monte Carlo package) web.ikp.kit.edu/rulrich/crmc.html

[14] A. Reinert and M. W. Winkler JCAP **1801** (2018) 055

[15] M. Korsmeier, F. Donato and M. Di Mauro, Phys. Rev. D **97** (2018) 103019

[16] A. Cuoco, *et al.* Phys. Rev. D **99** (2019) 103014

[17] M. Boudaud *et al.* arXiv:1906.07119

[18] M. Kachelriess, I. V. Moskalenko, and S. S. Ostapchenko Astrophys. J. **803** (2015) 54

[19] LHCb collaboration CERN-LHCC-2012-007

[20] LHCb collaboration CERN-LHCC-2019-0051

[21] A. Aab *et al.* (Pierre Auger Collaboration) Phys. Rev. D **91** (2015) 032003 Erratum: [ibid. **91** (2015) 059901]